

Directly Probing the Higgs-top Coupling at High Scales

Roshan Mammen Abraham and Dorival Gonçalves

Department of Physics, Oklahoma State University, Stillwater, OK, 74078, USA

Tao Han, Sze Ching Iris Leung, and Han Qin

PITT PACC, Department of Physics and Astronomy,

University of Pittsburgh, 3941 O'Hara St., Pittsburgh, PA 15260, USA

We explore the sensitivity to new physics for the coupling of the Higgs boson (h) and top quark (t) at high energy scales with the process $pp \rightarrow t\bar{t}h$ at the high-luminosity LHC. This process probes the coupling in both the space-like and time-like domains at a high scale, complementary to the off-shell Higgs processes in the time-like domain. The effects from physics beyond the Standard Model are parametrized in terms of the effective field theory framework and a non-local Higgs-top form factor. Focusing on the boosted Higgs regime in association with jet substructure techniques, we show that the present search can directly probe the Higgs-top coupling to good precision, providing a strong sensitivity to the new physics scale.

I. INTRODUCTION

The top-quark Yukawa coupling (y_t) is the strongest interaction of the Higgs boson in the Standard Model (SM) with $y_t \sim 1$. Owing to its magnitude, it plays a central role in Higgs phenomenology in the SM and could be most sensitive to physics beyond the Standard Model (BSM) associated with the electroweak symmetry breaking [1]. It is crucial for the stability of the SM vacuum during the electroweak phase transition in the early universe [2, 3]. It yields the largest quantum correction to the Higgs boson mass and can trigger the electroweak symmetry breaking in many well-motivated new physics scenarios [4–9]. Thus, the precise measurement of y_t can be fundamental to pin down possible new physics effects.

The top-quark Yukawa coupling has been determined indirectly at the LHC from the Higgs discovery channel $gg \rightarrow h$ via the top-quark loop [10]. It can also be directly measured via top pair production in association with a Higgs boson, $t\bar{t}h$. The observation of this channel was reported in 2018 by both ATLAS and CMS collaborations, with respective significances of 6.3 and 5.2 standard deviations [11, 12]. These measurements confirm the SM expectation that the Higgs boson interacts with the top-quark with an order one Yukawa coupling. The high-luminosity LHC (HL-LHC) projections indicate that the top Yukawa will be probed to a remarkable precision at the end of the LHC run, reaching an accuracy of $\delta y_t \lesssim \mathcal{O}(4)\%$ [13].

The current measurements are performed near the electroweak scale $Q \sim v$. If the new physics scale Λ is significantly larger than the energy probed at the LHC, the BSM effects generally scale as $(Q/\Lambda)^n$ with $n \geq 0$ [14–16], before reaching a new resonance. Therefore, it is desirable to enhance the new physics effects by exploring the high energy regime associated with the Higgs physics. Proposals have been made recently to study the off-shell Higgs signals $gg \rightarrow h^* \rightarrow VV$ [17–23]. This process could be sensitive to potential new physics of the $t\bar{t}h^*$ and VVh^* interactions or an h^* propagation at high

energy scales $Q > v$.

In the present study, we *directly* explore the Higgs-top coupling at high energy scales using the $t\bar{t}h$ production channel. For an on-shell Higgs production with high transverse momentum, this process effectively probes the top-quark Yukawa interaction at a high scale in both the space-like and time-like regimes. In contrast, the off-shell Higgs physics probes the complementary physics only in the time-like domain [21–23]. As a concrete formulation, we study the BSM effects to the Higgs-top Yukawa in the Effective Field Theory (EFT) framework, focusing on two relevant higher dimensional contributions. Then, we move on to a BSM hypothesis that features a non-local momentum-dependent form factor of the Higgs-top interaction [22, 23]. This form factor generally captures the top Yukawa composite substructure. To combine the large event yield with a high energy physics probe, we focus on the channel with the largest Higgs decay branching fraction, $\mathcal{BR}(h \rightarrow b\bar{b}) \sim 58\%$, in association with jet substructure techniques at the boosted Higgs regime.

The rest of the presentation is organized as follows. In Section II, we present the theoretical parameterization associated with the potential new physics for the Higgs-top couplings in the EFT framework and an interaction form factor. We then derive the new physics sensitivity to those interactions in Section III, featuring the effects that benefit with the energy enhancement at the boosted Higgs regime. Finally, we present a summary in Section IV.

II. NEW PHYSICS PARAMETRIZATION

A. Effective Field Theory

The Standard Model Effective Field Theory (SMEFT) provides a consistent bottom-up framework to search for new physics [15, 16, 20, 24–27]. In this scenario, the beyond the SM particles are too heavy to be produced on-shell. The new states can be integrated out and

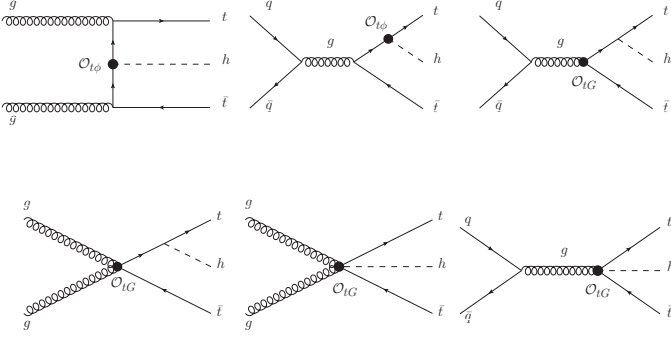


FIG. 1. Representative Feynman diagrams contributing to $t\bar{t}h$ production. The black dots represent the BSM vertices arising from the EFT operators.

parametrized in terms of higher dimension operators as contact interactions [14]. In general, the EFT Lagrangian can be written as

$$\mathcal{L}_{\text{EFT}} = \mathcal{L}_{\text{SM}} + \sum_i \frac{c_i}{\Lambda^2} \mathcal{O}_i + \mathcal{O}\left(\frac{1}{\Lambda^4}\right), \quad (1)$$

where Λ is the scale of new physics, \mathcal{O}_i are effective operators of dimension-six compatible with the SM symmetries, and c_i are corresponding Wilson coefficients. Higher dimensional operators can modify the existing SM interactions, as well as generate new Lorentz structures, both of which can give rise to phenomenologically relevant energy enhancements in the scattering amplitudes.

We follow the SMEFT framework to study the new physics effects to the Higgs-top coupling at high scales. We adopt the Warsaw basis of operators [16] and focus on two-fermion operators, leading to contributions to $t\bar{t}h$ production at the LHC which are relatively unconstrained

$$\mathcal{O}_{t\phi} = (H^\dagger H)(\bar{Q}t)\tilde{H} + \text{h.c.}, \quad (2)$$

$$\mathcal{O}_{tG} = g_s(\bar{Q}\sigma^{\mu\nu}T_A t)\tilde{H}G_{\mu\nu}^A + \text{h.c.} \quad (3)$$

The first new physics operator, $\mathcal{O}_{t\phi}$, rescales the SM top Yukawa coupling. The second one, \mathcal{O}_{tG} , corresponds to the chromomagnetic dipole moment of the top-quark. Besides modifying the $g\bar{t}t$ vertex in the SM, \mathcal{O}_{tG} also gives rise to new interaction vertices, namely $gg\bar{t}t$, $gt\bar{t}h$ and $gg\bar{t}h$. While \mathcal{O}_{tG} results in phenomenological effects to the associated $t\bar{t}$ processes, it amounts in possibly significant new physics sensitivity in the $t\bar{t}h$ channel [28]. Hence, we incorporate it in our analysis exploring its high energy behavior. In Fig. 1, we present a representative set of Feynman diagrams for $t\bar{t}h$ production arising from the EFT interactions. The experimental LHC analyses constrain these Wilson coefficients at 95% Confidence Level (CL) to the ranges [29, 30]

$$c_{t\phi}/\Lambda^2 = [-2.3, 3.1]/\text{TeV}^2, \quad c_{tG}/\Lambda^2 = [-0.24, 0.07]/\text{TeV}^2.$$

Guided by these results, we choose illustrative values of the coefficients as

$$|c_{tG}/\Lambda^2| = 0.1 \text{ TeV}^{-2} \quad \text{and} \quad |c_{t\phi}/\Lambda^2| = 1 \text{ TeV}^{-2}, \quad (4)$$

for our following representative kinematic distributions. For recent phenomenological SMEFT global fit studies, see Refs. [24, 25].

B. Higgs-Top coupling form-factor

The top-quark Yukawa coupling has a special role in the naturalness problem, displaying the dominant quantum corrections to the Higgs mass. Thus, it is crucially important to probe the Higgs-top interaction at high scales into the ultra-violet regime. It is well-motivated to consider that the top-quark and Higgs boson may not be fundamental, but composite particles arising from strongly interacting new dynamics at a scale Λ [7, 9, 31]. In such scenarios, the top Yukawa may exhibit a momentum-dependent form-factor near or above the new physics scale Λ , rather than a point-like interaction. It is challenging to write a form-factor, in a general form, without prior knowledge of the underlying strong dynamics of the specific composite scenario. Inspired by the nucleon form-factor [32], we adopt the following phenomenological ansatz

$$\Gamma(Q^2/\Lambda^2) = \frac{1}{(1 + Q^2/\Lambda^2)^n}, \quad (5)$$

where Q is the energy scale associated with the physical process. This educated guess results in a dipole form-factor for the $n = 2$ scenario with an exponential spatial distribution in a space-like probe. Higher values of n correspond to higher multi-poles, typically leading to a stronger suppression.

III. ANALYSIS

To probe these new physics contributions, we explore the $pp \rightarrow t\bar{t}h$ channel at high energy scales. We combine the large signal event rate with controlled backgrounds, studying the boosted $h \rightarrow b\bar{b}$ final state in association with leptonic top-quark pair decays. The signal is defined in the four b -tag sample and displays two opposite sign leptons. The leading backgrounds, in order of relevance, are $t\bar{t}b\bar{b}$ and $t\bar{t}Z$.

We perform the signal and background event generation with **MadGraph5_aMC@NLO** [33]. The $t\bar{t}h$ and $t\bar{t}Z$ samples are generated at NLO QCD and the $t\bar{t}b\bar{b}$ sample at LO. The dimension-six EFT contributions are added through the FeynRules model **SMEFT@NLO** [34]. This implementation grants one-loop QCD computations accounting for the EFT contributions. In particular, it incorporates relevant extra radiation effects at the matrix

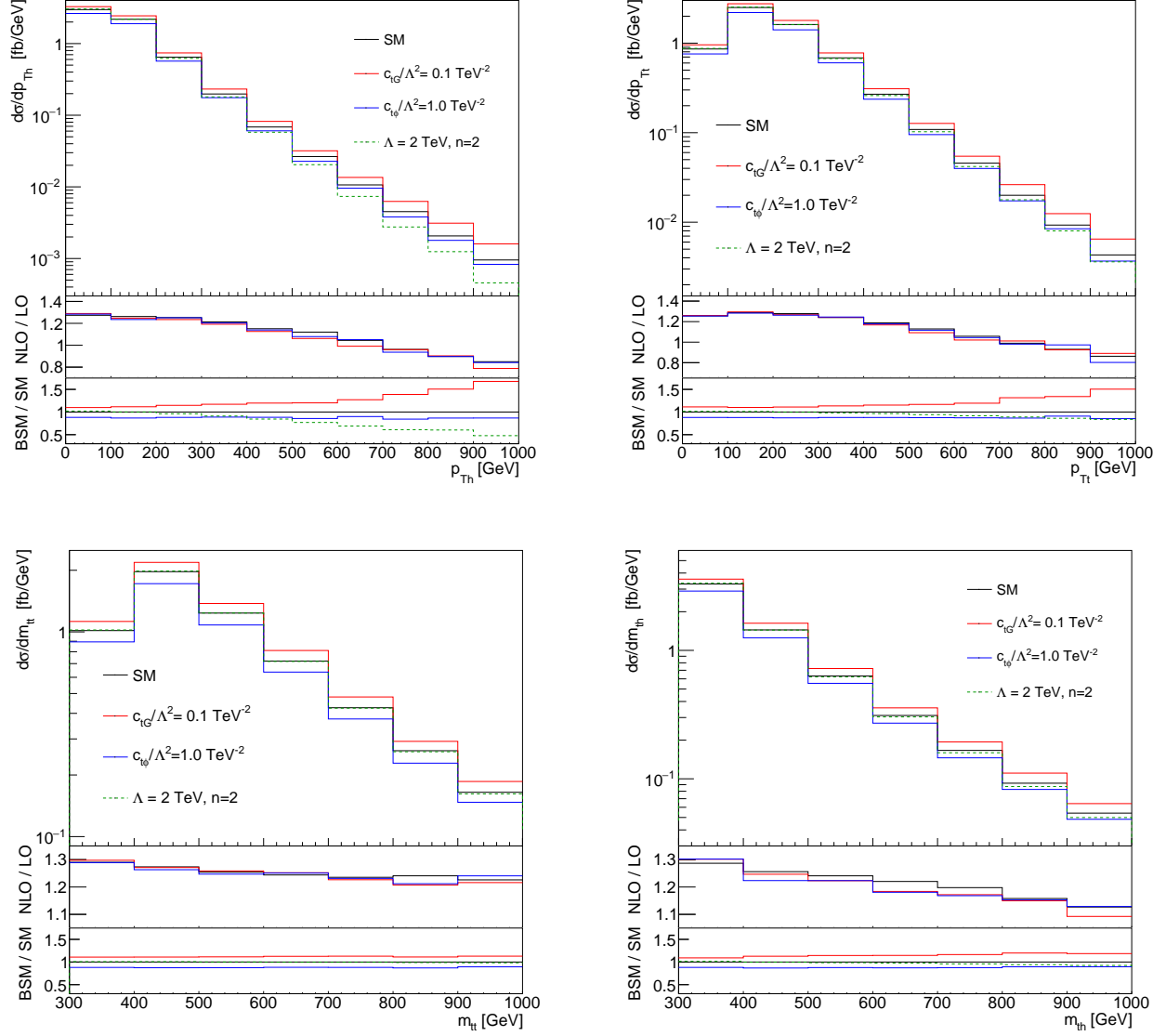


FIG. 2. Top panels: Transverse momentum distributions for the Higgs boson p_{T_h} (left) and the hardest top-quark p_{T_t} (right). Bottom panels: Invariant mass distributions for the top pair m_{tt} (left) and the Higgs and top-quark m_{th} (right). Each panel shows on the top the $t\bar{t}h$ sample in the SM and new physics scenarios. The results are presented at the NLO QCD fixed order. We also show the NLO K -factor (middle panel in each figure as NLO/LO) and the ratio between new physics and SM scenarios (bottom panel in each figure as BSM/SM). We assume the LHC at 14 TeV.

element level [35]. Shower, hadronization, and underlying event effects are simulated with `Pythia8` [36]. We use `MadSpin` to properly describe the top-quark decays, accounting for spin correlation effects [37]. We assume the LHC at $\sqrt{s} = 14$ TeV.

Robust new physics studies at the LHC usually come hand in hand with precise theoretical calculations. The impact of the higher order QCD corrections, which can be conventionally estimated by a K -factor (*i.e.* the ratio between the NLO and LO predictions), usually result in significant contributions. To illustrate the higher order and new physics effects at high energies, we present

in Fig. 2 the NLO fixed order parton level distribution for several relevant kinematic observables associated with the $t\bar{t}h$ signal sample: the transverse momentum distribution for the Higgs boson p_{T_h} (upper left), for the hardest top-quark p_{T_t} (upper right), the invariant mass distribution for the top pair m_{tt} (lower left), and for the Higgs and top-quark m_{th} (lower right). We observe that the higher order QCD corrections are correlated with the kinematic observables, resulting in about 20%–30% variation (as seen in the panels of NLO/LO) and cannot be captured by a global NLO K -factor. It is thus crucial to include the higher order predictions in the full dif-

ferential analysis. The factorization and renormalization scales were set to $\mu_F = \mu_R = m_t + m_h/2$.

New physics contributions may sensitively depend on the kinematics as well, as demonstrated in the panels of BSM/SM in Fig. 2. High transverse momenta of an on-shell top quark or Higgs boson could probe the space-like regime for the top-Higgs interactions, while the high invariant mass of the $t\bar{t}H$ system could be sensitive to the time-like regime from heavy states in s -channels. First, we observe sizable energy enhancement arising from the \mathcal{O}_{tG} operator, in particular, for the transverse Higgs momentum distribution (as seen in the panels of BSM/SM), starting with a 10% increase at the non-boosted regime $p_{Th} < 100$ GeV, adding up to 65% for $p_{Th} = 1$ TeV. In contrast, due to the generic dipole suppression, the form-factor scenario displays a depletion in cross-section at higher energies. The rate is reduced by 5% at $p_{Th} = 200$ GeV, reaching 55% suppression at $p_{Th} = 1$ TeV. For the form-factor scenario, we adopt a representative scale $Q = p_{Th}$. New physics effects associated with the operator $\mathcal{O}_{t\phi}$ do not result in a distinct energy profile with respect to the SM. In the $t\bar{t}h$ process, this operator only contributes with a shift to the top Yukawa, resulting in a flat rescale with respect to the SM cross-section, independent of the process energy scale. Despite the absence of a manifest energy enhancement, this new physics contribution can also benefit from our high energy scale analysis due to more controlled backgrounds at the boosted Higgs regime, as we will show in the following.

The boosted Higgs analysis, in combination with jet substructure techniques effectively suppress the initially overwhelming backgrounds for the $t\bar{t}h$ signal with the dileptonic top decays and $h \rightarrow b\bar{b}$, as first shown in Ref. [38]. Here we follow a similar strategy. We start

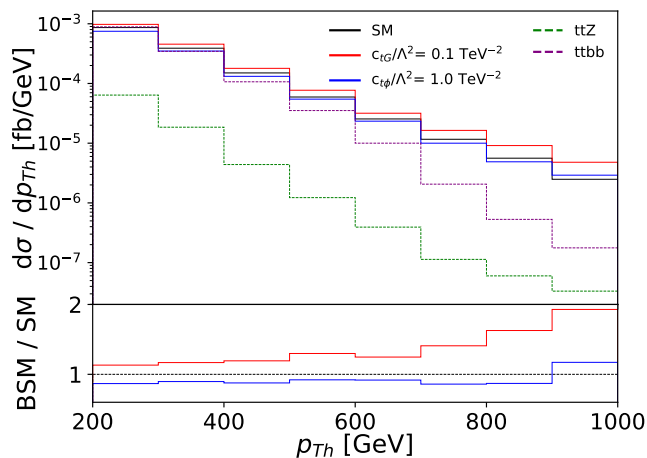


FIG. 3. Transverse momentum distribution of the Higgs boson p_{Th} for the $t\bar{t}h$ sample in the SM (black) and new physics scenarios with $c_{tG}/\Lambda^2 = 0.1$ TeV^{-2} (red), $c_{tG}/\Lambda^2 = 1$ TeV^{-2} (blue). The leading backgrounds $t\bar{t}b\bar{b}$ (purple) and $t\bar{t}Z$ (green) are also presented. We assume the LHC at 14 TeV.

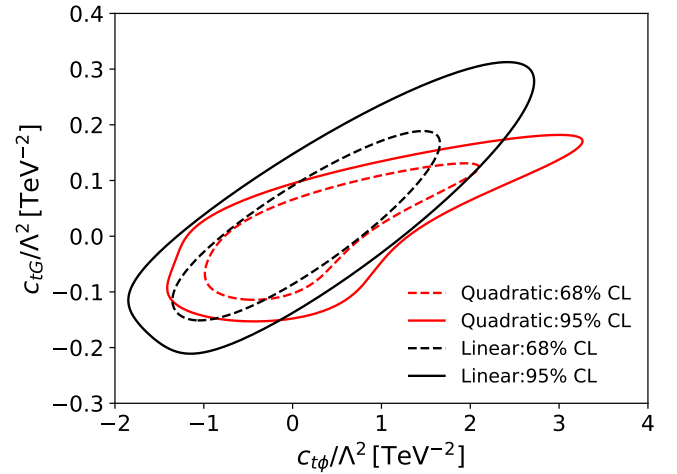


FIG. 4. 95% and 68% CL limits on the Wilson coefficients ($c_{tG}/\Lambda^2, c_{t\phi}/\Lambda^2$) at the 14 TeV HL-LHC with 3 ab^{-1} of data. The results are presented both at the linear and quadratic order in dimension-6 SMEFT operator coefficients.

our analysis requiring two isolated and opposite sign leptons with $p_{T\ell} > 10$ GeV and $|\eta_\ell| < 3$. For the hadronic component of the event, we first reconstruct jets with the Cambridge-Aachen algorithm with $R = 1.2$ [39], requiring at least one boosted fat-jet with $p_{TJ} > 200$ GeV and $|\eta_J| < 3$. We demand that one of the fat-jets be Higgs tagged with the Butterworth-Davison-Rubins-Salam (BDRS) algorithm [40, 41]. Among the three filtered jets, the two hardest are required to be b -tagged. As our final state displays in total four b -tagged jets, we exploit the improvements in the central tracking system, that will be in operation for the HL-LHC run, to enhance the event rate for our signal. Based on the ATLAS report [42], we assume 85% b -tagging efficiency and 1% mistag rate for light-jets.

As we only have one hadronic heavy particle decay, namely the Higgs boson, we proceed with the event reconstruction using a smaller jet size to further reduce the underlying event contamination. Thus, we remove all the hadronic activity associated with the Higgs fat-jet and re-cluster the remaining particles with the jet radius $R = 0.4$, using the anti- k_t jet algorithm. We demand two b -tagged jets with $p_{tb} > 30$ GeV and $|\eta_b| < 3$. To further suppress the backgrounds, the filtered mass for the Higgs candidate is imposed to be around the Higgs boson mass $|m_h^{\text{BDRS}} - 125 \text{ GeV}| < 10 \text{ GeV}$. We show in Table I more details on the cut-flow analysis.

A. Scale for the EFT operators

In Fig. 3, we go beyond the partonic level calculation and display the hadron level transverse momentum distribution (p_{Th}) for the Higgs boson candidate from the $pp \rightarrow t\bar{t}h$ channel in the SM and the EFT contribu-

cuts	$t\bar{t}h$	$t\bar{t}b\bar{b}$	$t\bar{t}Z$
BDRS h -tag, $p_{T\ell} > 10$ GeV, $ \eta_\ell < 3$, $n_\ell = 2$	3.32	6.35	1.02
$p_{Tj} > 30$ GeV, $ \eta_j < 3$, $n_j \geq 2$, $n_b = 2$	0.72	1.97	0.22
$ m_h^{\text{BDRS}} - 125 < 10$ GeV	0.15	0.14	0.009

TABLE I. Cut-flow for signal and backgrounds at LHC $\sqrt{s} = 14$ TeV. The selection follows the BDRS analysis described in the text. Rates are in units of fb and account for 85% (1%) b -tag (mistag) rate, hadronization, and underlying event effects.

tions, in addition to the leading backgrounds $t\bar{t}b\bar{b}$ and $t\bar{t}Z$. We observe that the boosted Higgs search dovetails nicely with our BSM physics study as presented in Fig. 2. At the higher energy scales, both the backgrounds get further depleted and the new physics effects become more prominent. In particular, we observe a large enhancement from the \mathcal{O}_{tG} contributions at the high energy scales.

To explore the sensitivity reach for these effects in the boosted regime, we perform a binned log-likelihood analysis on the p_{Th} distribution. In Fig. 4, we present the 68% and 95% CL limits on the Wilson coefficients ($c_{tG}/\Lambda^2, c_{t\phi}/\Lambda^2$). We assume the HL-LHC at 14 TeV with 3 ab^{-1} of data. To infer the uncertainty on the EFT expansion, we present the results accounting for terms up to linear and quadratic order on the Wilson coefficient c_i/Λ^2 . We observe only small differences between these two scenarios which is a good indication of the robustness of our results.

CMS has recently reported an EFT interpretation using associated top quark production data with an integrated luminosity of $\mathcal{L} = 41.5 \text{ fb}^{-1}$ [43]. The signal samples include, in particular, the $t\bar{t}h$ and thq processes, being direct sensitive to the top-quark Yukawa

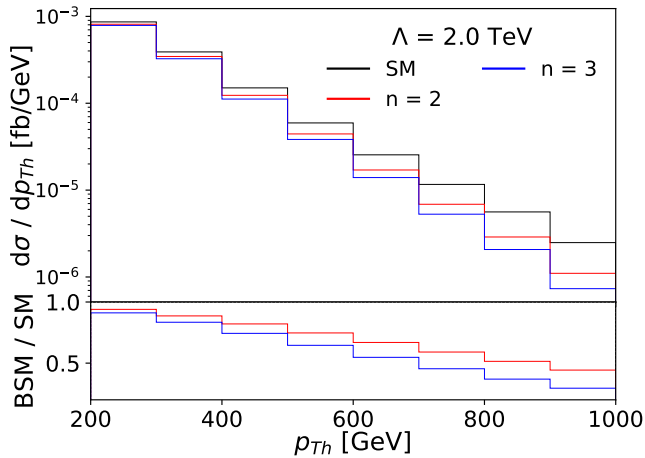


FIG. 5. Transverse momentum distribution of the Higgs boson p_{Th} for the $t\bar{t}h$ sample in the SM (black) and new physics scenarios with $n = 2$ (red) and $n = 3$ (blue), assuming $\Lambda = 2$ TeV. We assume the LHC at 14 TeV.

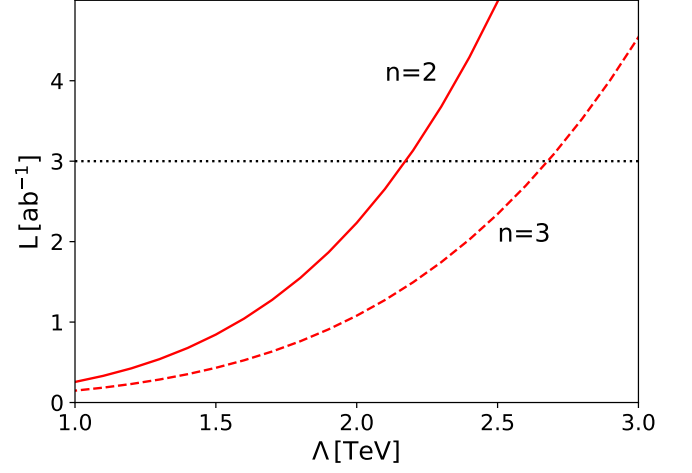


FIG. 6. 95% CL sensitivity on the new physics scale Λ as a function of the LHC luminosity. We consider two form-factor scenarios: $n = 2$ (solid line) and $n = 3$ (dashed line).

coupling. The resulting constraint at the 95% CL for the chromomagnetic operator leads to two regions $c_{tG}/\Lambda^2 = [-1.26, -0.69] \text{ TeV}^{-2}$ and $[0.08, 0.79] \text{ TeV}^{-2}$. The same holds for the $\mathcal{O}_{t\phi}$ operator where $c_{t\phi} = [-14.12, -1.46] \text{ TeV}^{-2}$ and $[32.30, 44.48] \text{ TeV}^{-2}$. While CMS does not focus on the very high energy scales and uses the leptonic Higgs decays, we explore the largest Higgs branching ratio, $h \rightarrow b\bar{b}$, in the boosted Higgs regime, and thus obtaining significantly higher sensitivities at the HL-LHC.

B. Probing the form-factor

In Fig. 5, we present the transverse momentum distribution (p_{Th}) for the Higgs boson candidate from the $pp \rightarrow t\bar{t}h$ channel in the SM and the form-factor contribution. We consider two hypotheses $n = 2$ and $n = 3$ with the new physics scale $\Lambda = 2$ TeV. While it is challenging to probe the BSM effects at relatively small scales, these contributions can be effectively enhanced at the boosted regime. For instance, starting at $p_{Th} \sim 200$ GeV with $n = 2$ ($n = 3$), we observe a 5% (9%) effect. Moving to $p_{Th} \sim 400$ GeV, the new physics results in larger depletion of 18% (25%) with respect to the SM hypothesis.

Our relatively large event rate with the boosted $h \rightarrow b\bar{b}$ analysis, grants probes at large energy scales with relevant statistics. Hence, we explore the full profile of the p_{Th} distribution through a binned log-likelihood analysis. The new physics sensitivity is presented in Fig. 6. The HL-LHC, with 3 ab^{-1} of data, will be able to probe these new physics effects up to a scale of $\Lambda = 2.1$ TeV for $n = 2$ and $\Lambda = 2.7$ TeV for $n = 3$ at 95% CL. These results are complementary to the off-shell Higgs analyses, $gg \rightarrow h^* \rightarrow ZZ$. For the latter, assuming $n = 3$, the limits on the new physics scale are $\Lambda = 1.1$ TeV for

	channel	c_i/Λ^2 [TeV $^{-2}$] 95% CL bounds	$\Lambda/\sqrt{c_i}$ [TeV] BSM scale
$c_{t\phi}$	$t\bar{t}h$ (this work)	$[-1.04, 1.00]$	1.0
	$h^* \rightarrow ZZ \rightarrow \ell\ell\nu\nu$ [23]	$[-2.8, 1.5]$	0.6
	$h^* \rightarrow ZZ \rightarrow 4\ell$ [22]	$[-3.3, 3.3]$	0.55
	Higgs comb. ATLAS [29]	$[-2.3, 3.1]$	0.57
c_{tG}	$t\bar{t}h$ (this work)	$[-0.11, 0.12]$	2.9
	$t\bar{t}$ CMS [30]	$[-0.24, 0.07]$	2.1
form-factor $n = 2$	$t\bar{t}h$ (this work)	-	2.1
	$h^* \rightarrow ZZ \rightarrow \ell\ell\nu\nu$ [23]	-	1.5
	$h^* \rightarrow ZZ \rightarrow 4\ell$ [22]	-	0.8
form-factor $n = 3$	$t\bar{t}h$ (this work)	-	2.7
	$h^* \rightarrow ZZ \rightarrow \ell\ell\nu\nu$ [23]	-	2.1
	$h^* \rightarrow ZZ \rightarrow 4\ell$ [22]	-	1.1

TABLE II. Summary results from the $t\bar{t}h$ studies for the Higgs-top coupling at high scales in terms of the dimension-6 operators and general form-factor scenarios. The results are shown at 95% CL, and we assume the HL-LHC at 14 TeV with 3 ab $^{-1}$ of data. For comparison, we also show the results from off-shell h^* studies, the ATLAS Higgs combination with 139 fb $^{-1}$, and the CMS top pair bound with 35.9 fb $^{-1}$.

the 4ℓ final state and $\Lambda = 2.1$ TeV for the $\ell\ell\nu\nu$ final state [22, 23].

IV. SUMMARY AND DISCUSSIONS

We studied the prospects to *directly* probe the Higgs-top coupling for new physics at high energy scales using the $pp \rightarrow t\bar{t}h$ process at the HL-LHC. We considered two beyond the SM scenarios, namely the SMEFT framework and a general Higgs-top form-factor, as discussed in Sec. II. We presented in Sec. III the general phenomenological effects for these new physics contributions, showing that they could produce augmented new physics effects at high energy scales.

Focusing on the boosted Higgs regime in association with jet substructure techniques, we explored the largest Higgs branching fraction $h \rightarrow b\bar{b}$ along with the clean leptonic top-quark decays. The BSM effects were constrained through a shape analysis on the p_{Th} spectrum. We observed the potential sensitivity at the TeV-scale for new physics both in the EFT and form-factor scenarios. The chromomagnetic dipole operator was probed up to $\Lambda/\sqrt{c_{tG}} \approx 2.9$ TeV and the $\mathcal{O}_{t\phi}$ operator to $\Lambda/\sqrt{c_{t\phi}} \approx 1.0$ TeV, as shown in Sec. III A. The limits presented sub-leading differences between the linear and quadratic c_i/Λ^2 expansion, indicating that our phenomenological study satisfies the EFT expansion. Finally, when considering a more general Higgs-top quark form-factor in Sec. III B, we concluded that the HL-LHC

is sensitive to new physics up to the scale $\Lambda = 2.1$ TeV for $n = 2$ and 2.7 TeV for $n = 3$ at 95% CL. Further details are summarized in Table II. The $t\bar{t}h$ studies at high scales, which *directly* explore the Higgs-top Yukawa interaction results in a competitive and complementary pathway for BSM sensitivity in comparison to the off-shell Higgs channels and the current ATLAS and CMS limits.

Some improvements of sensitivity can be anticipated by including other modes such as $t\bar{t}(h \rightarrow \gamma\gamma)$, which would yield a cleaner signal but a lower rate. In addition, we can increase our present $t\bar{t}(h \rightarrow b\bar{b})$ statistical sample by about a factor of six, if we include one leptonic decay plus one hadronic decay of the $t\bar{t}$. The analysis, however, would be more complex, with significantly larger QCD backgrounds [44]. We leave those improvements to future work with realistic simulations.

ACKNOWLEDGMENTS

RMA and DG thank the U.S. Department of Energy for the financial support, under grant number DE-SC 0016013. The work of TH, SCIL, and HQ is supported by the U.S. Department of Energy under grant No. DE-FG02-95ER40896 and by the PITT PACC. Some of the computing for this project was performed at the High Performance Computing Center at Oklahoma State University supported in part through the National Science Foundation grant OAC-1531128.

-
- [1] Christopher T. Hill and Elizabeth H. Simmons. Strong Dynamics and Electroweak Symmetry Breaking. *Phys. Rept.*, 381:235–402, 2003. [Erratum: *Phys.Rept.* 390, 553–554 (2004)].
- [2] Dario Buttazzo, Giuseppe Degrandi, Pier Paolo Gia-

- rdino, Gian F. Giudice, Filippo Sala, Alberto Salvio, and Alessandro Strumia. Investigating the near-criticality of the Higgs boson. *JHEP*, 12:089, 2013.
- [3] Fedor Bezrukov and Mikhail Shaposhnikov. Why should we care about the top quark Yukawa coupling? *J. Exp.*

- Theor. Phys.*, 120:335–343, 2015.
- [4] Marcela Carena, M. Olechowski, S. Pokorski, and C. E. M. Wagner. Radiative electroweak symmetry breaking and the infrared fixed point of the top quark mass. *Nucl. Phys. B*, 419:213–239, 1994.
 - [5] Giuliano Panico and Andrea Wulzer. The Discrete Composite Higgs Model. *JHEP*, 09:135, 2011.
 - [6] Oleksii Matsedonskyi, Giuliano Panico, and Andrea Wulzer. Light Top Partners for a Light Composite Higgs. *JHEP*, 01:164, 2013.
 - [7] Alex Pomarol and Francesco Riva. The Composite Higgs and Light Resonance Connection. *JHEP*, 08:135, 2012.
 - [8] Brando Bellazzini, Csaba Csáki, and Javi Serra. Composite Higgses. *Eur. Phys. J. C*, 74(5):2766, 2014.
 - [9] Giuliano Panico and Andrea Wulzer. *The Composite Nambu-Goldstone Higgs*, volume 913. Springer, 2016.
 - [10] Georges Aad et al. Combined measurements of Higgs boson production and decay using up to 80 fb⁻¹ of proton-proton collision data at $\sqrt{s} = 13$ TeV collected with the ATLAS experiment. *Phys. Rev. D*, 101(1):012002, 2020.
 - [11] M. Aaboud et al. Observation of Higgs boson production in association with a top quark pair at the LHC with the ATLAS detector. *Phys. Lett. B*, 784:173–191, 2018.
 - [12] Albert M Sirunyan et al. Observation of $t\bar{t}H$ production. *Phys. Rev. Lett.*, 120(23):231801, 2018.
 - [13] M. Cepeda et al. Report from Working Group 2: Higgs Physics at the HL-LHC and HE-LHC. *CERN Yellow Rep. Monogr.*, 7:221–584, 2019.
 - [14] Thomas Appelquist and J. Carazzone. Infrared Singularities and Massive Fields. *Phys. Rev. D*, 11:2856, 1975.
 - [15] W. Buchmuller and D. Wyler. Effective Lagrangian Analysis of New Interactions and Flavor Conservation. *Nucl. Phys. B*, 268:621–653, 1986.
 - [16] B. Grzadkowski, M. Iskrzynski, M. Misiak, and J. Rosiek. Dimension-Six Terms in the Standard Model Lagrangian. *JHEP*, 10:085, 2010.
 - [17] Aleksandr Azatov, Christophe Grojean, Ayan Paul, and Ennio Salvioni. Taming the off-shell Higgs boson. *Zh. Eksp. Teor. Fiz.*, 147:410–425, 2015.
 - [18] Christoph Englert and Michael Spannowsky. Limitations and Opportunities of Off-Shell Coupling Measurements. *Phys. Rev. D*, 90:053003, 2014.
 - [19] Malte Buschmann, Dorival Gonçalves, Silvan Kuttimalai, Marek Schonherr, Frank Krauss, and Tilman Plehn. Mass Effects in the Higgs-Gluon Coupling: Boosted vs Off-Shell Production. *JHEP*, 02:038, 2015.
 - [20] Tyler Corbett, Oscar J. P. Eboli, Dorival Gonçalves, J. Gonzalez-Fraile, Tilman Plehn, and Michael Rauch. The Higgs Legacy of the LHC Run I. *JHEP*, 08:156, 2015.
 - [21] Dorival Gonçalves, Tao Han, and Satyanarayan Mukhopadhyay. Off-Shell Higgs Probe of Naturalness. *Phys. Rev. Lett.*, 120(11):111801, 2018. [Erratum: *Phys.Rev.Lett.* 121, 079902 (2018)].
 - [22] Dorival Gonçalves, Tao Han, and Satyanarayan Mukhopadhyay. Higgs Couplings at High Scales. *Phys. Rev. D*, 98(1):015023, 2018.
 - [23] Dorival Gonçalves, Tao Han, Sze Ching Iris Leung, and Han Qin. Off-shell Higgs Couplings in $H^* \rightarrow ZZ \rightarrow \ell\ell\nu\nu$. 12 2020.
 - [24] John Ellis, Maeve Madigan, Ken Mimasu, Veronica Sanz, and Tevong You. Top, Higgs, Diboson and Electroweak Fit to the Standard Model Effective Field Theory. 12 2020.
 - [25] Jacob J. Ethier, Fabio Maltoni, Luca Mantani, Emanuele R. Nocera, Juan Rojo, Emma Slade, Eleni Vryonidou, and Cen Zhang. Combined SMEFT interpretation of Higgs, diboson, and top quark data from the LHC. 4 2021.
 - [26] Ilaria Brivio, Sebastian Bruggisser, Fabio Maltoni, Rhea Moutafis, Tilman Plehn, Eleni Vryonidou, Susanne Westhoff, and C. Zhang. O new physics, where art thou? A global search in the top sector. *JHEP*, 02:131, 2020.
 - [27] Anke Biekötter, Dorival Gonçalves, Tilman Plehn, Michihisa Takeuchi, and Dirk Zerwas. The global Higgs picture at 27 TeV. *SciPost Phys.*, 6(2):024, 2019.
 - [28] Fabio Maltoni, Eleni Vryonidou, and Cen Zhang. Higgs production in association with a top-antitop pair in the Standard Model Effective Field Theory at NLO in QCD. *JHEP*, 10:123, 2016.
 - [29] A combination of measurements of Higgs boson production and decay using up to 139 fb⁻¹ of proton-proton collision data at $\sqrt{s} = 13$ TeV collected with the ATLAS experiment. Technical report, CERN, Geneva, Aug 2020.
 - [30] Albert M Sirunyan et al. Measurement of the top quark polarization and $t\bar{t}$ spin correlations using dilepton final states in proton-proton collisions at $\sqrt{s} = 13$ TeV. *Phys. Rev. D*, 100(7):072002, 2019.
 - [31] Da Liu, Ian Low, and Carlos E. M. Wagner. Modification of Higgs Couplings in Minimal Composite Models. *Phys. Rev. D*, 96(3):035013, 2017.
 - [32] V. Punjabi, C. F. Perdrisat, M. K. Jones, E. J. Brash, and C. E. Carlson. The Structure of the Nucleon: Elastic Electromagnetic Form Factors. *Eur. Phys. J. A*, 51:79, 2015.
 - [33] J. Alwall, R. Frederix, S. Frixione, V. Hirschi, F. Maltoni, O. Mattelaer, H. S. Shao, T. Stelzer, P. Torrielli, and M. Zaro. The automated computation of tree-level and next-to-leading order differential cross sections, and their matching to parton shower simulations. *JHEP*, 07:079, 2014.
 - [34] Céline Degrande, Gauthier Durieux, Fabio Maltoni, Ken Mimasu, Eleni Vryonidou, and Cen Zhang. Automated one-loop computations in the SMEFT. 8 2020.
 - [35] Reza Goldouzian, Jeong Han Kim, Kevin Lannon, Adam Martin, Kelci Mohrman, and Andrew Wightman. Matching in $pp \rightarrow t\bar{t}W/Z/h + \text{jet}$ SMEFT studies. 12 2020.
 - [36] Torbjorn Sjostrand, Stephen Mrenna, and Peter Z. Skands. A Brief Introduction to PYTHIA 8.1. *Comput. Phys. Commun.*, 178:852–867, 2008.
 - [37] Pierre Artoisenet, Rikkert Frederix, Olivier Mattelaer, and Robbert Rietkerk. Automatic spin-entangled decays of heavy resonances in Monte Carlo simulations. *JHEP*, 03:015, 2013.
 - [38] Matthew R. Buckley and Dorival Gonçalves. Boosting the Direct CP Measurement of the Higgs-Top Coupling. *Phys. Rev. Lett.*, 116(9):091801, 2016.
 - [39] Matteo Cacciari, Gavin P. Salam, and Gregory Soyez. FastJet User Manual. *Eur. Phys. J. C*, 72:1896, 2012.
 - [40] Jonathan M. Butterworth, Adam R. Davison, Mathieu Rubin, and Gavin P. Salam. Jet substructure as a new Higgs search channel at the LHC. *Phys. Rev. Lett.*, 100:242001, 2008.
 - [41] Tilman Plehn, Gavin P. Salam, and Michael Spannowsky. Fat Jets for a Light Higgs. *Phys. Rev. Lett.*, 104:111801, 2010.
 - [42] Technical Design Report for the ATLAS Inner Tracker Pixel Detector. Technical Report CERN-LHCC-2017-

021. ATLAS-TDR-030, CERN, Geneva, Sep 2017.
- [43] Using associated top quark production to probe for new physics within the framework of effective field theory. Technical report, CERN, Geneva, 2020.
- [44] Morad Aaboud et al. Search for the standard model Higgs boson produced in association with top quarks and decaying into a $b\bar{b}$ pair in pp collisions at $\sqrt{s} = 13$ TeV with the ATLAS detector. *Phys. Rev. D*, 97(7):072016, 2018.